**TABLE 1.** Demographics of Highly Myopic Patients With and Without Patchy Chorioretinal Atrophy

| | With Patchy Atrophy | Without Patchy Atrophy | P Value |
|---|---|---|---|
| Sex, no. eyes (persons) | | | |
| Men | 13 (11) | 24 (17) | n.s. |
| Women | 43 (33) | 89 (52) | |
| Age (y), mean ± SD (range) | 60.9 ± 12.8 (30~85) | 61.3 ± 14.3 (18~85) | n.s. |
| Refractive error (diopters), mean ± SD (range) | −13.7 ± 4.0 (−8.5~−20.0) | −13.0 ± 3.6 (−8.5~−20.0) | n.s. |
| Axial length (mm), mean ± SD (range) | 30.2 ± 1.8 (26.5~35.3) | 29.3 ± 1.8 (26.5~35.0) | .003[a] |
| Number of patchy atrophy per eye, mean ± SD (range) | 1.9 ± 1.1 (1~6) | N/A | |

n.s. = not significant; SD = standard deviation; y = years.
[a]Student t test and Welch t test.
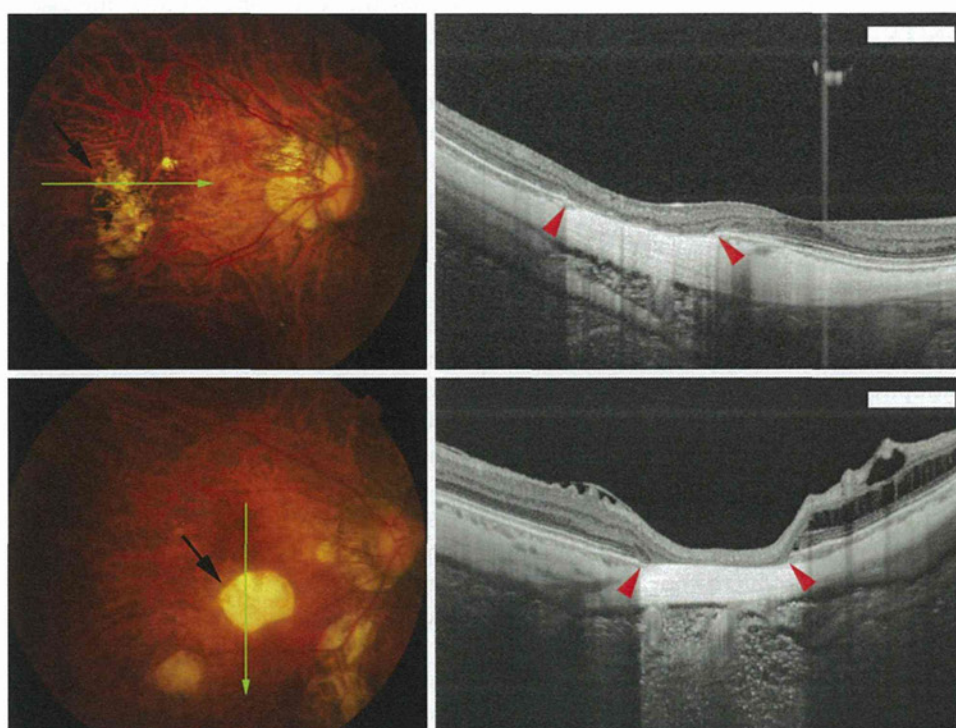


FIGURE 1. Swept-source optical coherence tomographic (OCT) images of highly myopic eyes with patchy chorioretinal atrophy without a change of the scleral curvature. (Top left) Right fundus of a 42-year-old woman shows patchy chorioretinal atrophy temporal to the fovea (arrow). The refractive error was −11.0 diopters and the axial length was 28.4 mm. (Top right) B-scan swept-source OCT image of the scanned line shown at top left shows that the outer retina, retinal pigment epithelium (RPE), and choroid are not present in the area of the patchy atrophy (between arrowheads). The inner retina is directly attached to the sclera. The inner and outer curvature of the sclera in the area of patchy atrophy is not different from the neighboring sclera. (Bottom left) Right fundus of a 56-year-old woman showing patchy chorioretinal atrophy located inferior to the fovea (arrow). Her refractive error was −13.0 diopters and the axial length was 29.7 mm. (Bottom right) B-scan swept-source OCT image of the scanned line shown at bottom left shows that the outer retina, RPE, and choroid are absent in the area of patchy atrophy (between arrowheads). The inner retina is directly attached to the sclera. The inner and outer curvature of the sclera in the area of patchy atrophy is not different from the neighboring sclera. Bar: 1 mm.

cavitations that develop adjacent to a myopic conus in highly myopic eyes and are referred to as peripapillary intrachoroidal cavitations. Peripapillary intrachoroidal cavitations are seen as yellowish-orange lesions located inferior to the optic disc and are found in 4.9% of highly myopic eyes.[15] This lesion was originally termed peripap-illary detachment in pathologic myopia[16] because the defect was thought to represent an elevation of the retina and the RPE. Toranzo and associates[17] used a Stratus 3000 OCT (Humphrey-Zeiss, Dublin, California, USA) and found that a deep hyporeflectivity area was present in the underlying choroid. They changed the name of the defect

to peripapillary intrachoroidal cavitation. We recently examined highly myopic patients with peripapillary intrachoroidal cavitation with a swept-source OCT and found that the sclera was bowed posteriorly under the region of the intrachoroidal cavitation, while the overlying retina-RPE–Bruch membrane complex showed little, if any, deformation.[13]

The purpose of this study was to determine the incidence and morphology of the intrachoroidal cavitations in the macular area in highly myopic eyes with patchy chorioretinal atrophy. The clinical significance of the lesions, especially their association with the development of retinoschisis, was also examined.

## PATIENTS AND METHODS

FORTY-FOUR CONSECUTIVE PATIENTS WITH PATHOLOGIC myopia and patchy chorioretinal atrophy[8] in the macula were studied. All of the patients were examined with a swept-source OCT from July 22, 2011 to October 14, 2011 in the High Myopia Clinic at Tokyo Medical and Dental University, Tokyo, Japan. The definition of pathologic myopia was a refractive error (myopic spherical equivalent) >8.00 diopters (D) or an axial length >26.5 mm. Sixty-eight consecutive patients with high myopia but without patchy atrophy who visited the High Myopia Clinic between July 22, 2011 and October 14, 2011 were also analyzed as controls. All of the participants had a comprehensive ocular examination including measurements of the refractive error (spherical equivalent), axial length with IOL Master (Carl Zeiss Meditec, Dublin, California, USA), and fundus biomicroscopy.

Patchy chorioretinal atrophy was defined as a well-defined grayish-white retinochoroidal lesion.[8] In the atrophic phase of myopic CNVs, well-defined chorioretinal atrophy can develop that resembles a patchy chorioretinal atrophy.[8,18,19] However, the atrophic phase of a myopic CNV is different from patchy atrophy, and the eyes with this lesion were excluded from this study. Also, patients who had undergone vitreoretinal surgeries, had poor fixation attributable to dense cataract, and had myopic macular holes were excluded. The area of patchy chorioretinal atrophy was determined from the color fundus photographs using software of an imaging system (PDT/MPS software; Topcon, Tokyo, Japan) that is based on the axial length, the corneal curvature, and the refractive power of the eye. This software uses Littmann's formula based on the values of the Gullstrand schematic eye.[20,21] Vertical and horizontal lines were drawn through the fovea on the photograph of each eye, and the location of patchy atrophy was divided into 4 quadrants: upper nasal, lower nasal, upper temporal, and lower temporal. One author (M.M.) masked to the OCT findings determined the location and measured the area of the patchy atrophy.

• SWEPT-SOURCE OPTICAL COHERENCE TOMOGRAPHY: All of the eyes were examined by a prototype swept-source OCT instrument manufactured by Topcon Corporation. This swept-source OCT system has an A-scan repetition rate of 100 000 Hz, and its light source operates in the 1-μm wavelength region. The light source is a wavelength-sweeping laser centered at 1050 nm with an approximate 100-nm tuning range. However, the effective bandwidth was approximately 60 nm because of the absorption of the energy by water. The axial resolution was calculated to be 8 μm in tissue with a lateral resolution of 20 μm. The imaging depth was 2.6 mm in tissue, and the lateral scan length was adjustable.

Four scanning protocols were used: 3-dimensional (3D) volumetric scans, line scans, 7-line raster scans, and radial scans. The 3D volumetric data were acquired in 0.8 seconds and each 3D scan covered an area of 6 × 6 mm$^2$ with a 256 (horizontal) × 256 (vertical) lines A-scan density. To improve the image quality, 3 consecutive B-scan images were averaged by a weighted moving average. The 7-line raster scans and radial scans were performed when necessary. Each scan had a lateral scan length of either 6 mm or 9 mm. A single image was made up of 1024 A lines acquired in 10 ms. Typically, 32 B-scan images were recorded and averaged by post-processing to yield a despeckled B-scan image. The width and depth of the intrachoroidal cavitation was measured with the built-in caliper function of the OCT software by 1 masked author (M.M.).

• STATISTICAL ANALYSES: The patients' age, axial length, and the size of the patchy atrophy were compared between eyes using Mann-Whitney U tests, paired t tests, and Welch t tests. The sex distribution was analyzed using $\chi^2$ tests. The incidence of peripapillary intrachoroidal cavitations or macular retinoschisis, and the locations of the intrachoroidal cavitations, were analyzed by $\chi^2$ tests. A P value <.05 was considered statistically significant.

## RESULTS

FIFTY-SIX EYES OF 44 CONSECUTIVE HIGHLY MYOPIC PA-tients with patchy atrophy that were examined by swept-source OCT in the High Myopia Clinic at Tokyo Medical and Dental University between July 22, 2011 and October 14, 2011 were studied. Thirty-two eyes were excluded because of unilateral high myopia, history of vitreoretinal surgery, dense cataracts, and poor fixation. The demographics of the 44 patients and 68 highly myopic patients (113 eyes) without patchy atrophy are shown in Table 1.

The average number of patchy atrophies was 1.9 ± 1.1/eye. A posterior staphyloma was found in all of the eyes with patchy atrophy and in 108 of 113 eyes without patchy atrophy. There was no significant difference in the age and refractive error between highly myopic eyes with and
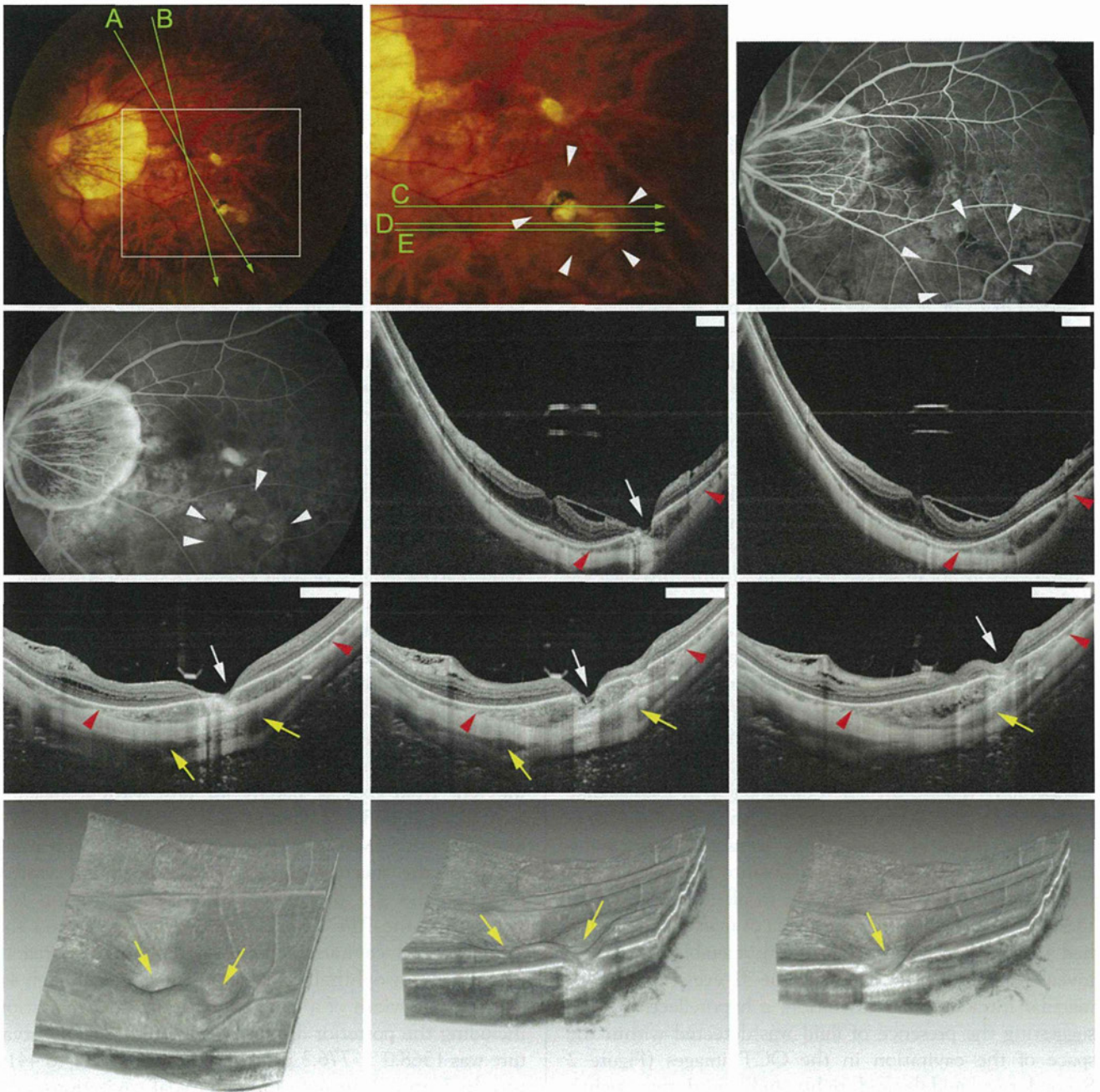
FIGURE 2. Intrachoroidal cavitation with a bowing of the sclera in and around the area of patchy chorioretinal atrophy. (Top left) Photograph of the left fundus of a 60-year-old woman showing 3 areas of patchy chorioretinal atrophy temporal to and inferotemporal to the fovea. (Top middle) Magnified image of top left image shows 3 areas of patchy chorioretinal atrophy. The area around the patchy atrophy is orange (arrowheads). (Top right) Fluorescein fundus angiographic image at 1 minute after dye injection shows relative hypofluorescence (arrowheads) around the patchy atrophy. (Second row, left) Fluorescein fundus angiographic image at 7 minutes after dye injection shows mild hyperfluorescence (arrowheads) around the patchy atrophy. (Second row, middle) B-scan swept-source optical coherence tomographic (OCT) image of line A in top left image shows that the sclera is bowed posteriorly (between arrowheads) compared to neighboring sclera beyond the retinal pigment epithelium (RPE) defects. The choroid seems to be thickened in the area and the retina is caved into the intrachoroidal cavitation (arrow). Inner retinoschisis is observed around the intrachoroidal cavitation. (Second row, right) In the section shown by line B in top left image, a bowing of the sclera is observed (between arrowheads). The hyporeflective space suggests the presence of fluid in the space of the intrachoroidal cavitation. (Third row, left) B-scan swept-source OCT image of the scanned line C in top middle image shows that the sclera is bowed posteriorly (between arrowheads) beyond the area of RPE defects. The retina is caved into the intrachoroidal cavitation and has a pseudo-fovea appearance (white arrow). Large intrascleral blood vessels (yellow arrows) are observed in close proximity to the intrachoroidal cavitation. (Third row, middle) In the section shown by line D in top middle image, the sclera is bowed posteriorly (between arrowheads) and large intrascleral vessels (yellow arrows) are observed in close proximity to the intrachoroidal cavitation.

without patchy atrophy (Table 1). The axial length was significantly longer in eyes with patchy atrophy than in those without patchy atrophy ($P = .003$, Student $t$ test and Welch $t$ test).

The examinations of the area of patchy chorioretinal atrophy by swept-source OCT showed that the outer retina, the RPE, and the choroid were absent, and the inner retina appeared to be attached directly to the sclera (Figure 1). However, the curvature of the inner and outer sclera in the area of patchy atrophy did not differ from that of the neighboring sclera (Figure 1). This type of OCT finding was observed in 23 of 56 eyes (41.1%) with patchy atrophy.

In the remaining 33 eyes with patchy atrophy, swept-source OCT showed that the sclera of these eyes was bowed more posteriorly than the surrounding area in 31 of the 56 eyes (55.4%; Figures 2 through 4). The morphologic appearance of these lesions in swept-source OCT images was strikingly similar to those of the peripapillary intrachoroidal cavitations found in eyes with pathologic myopia.[13,15−17,22] The only difference was in the location, that is, peripapillary vs macular. A macular intrachoroidal cavitation was not observed in the 113 highly myopic eyes without patchy atrophy.

Funduscopic examination showed that the macular intrachoroidal cavitation appeared as an orange-colored lesion with ill-defined borders surrounding the patchy atrophy (Figures 2 and 3) in 14 of 31 eyes (45.2%). The region was mildly hypofluorescent in the early phase and slightly hyperfluorescent in the late phase of fluorescein angiography (Figure 2). The orange color in funduscopic examination and fluorescein angiographic findings were similar to those of peripapillary intrachoroidal cavitation.[13,15−17] The retina was sunken into the space of the macular intrachoroidal cavitation in all eyes. Because of the caving-in of the retina, the area of macular cavitation had a dented appearance, and this site resembled a "pseudofovea" (Figures 2 and 3). In 3 of the 31 eyes (9.7%) with macular intrachoroidal cavitation, a hyporeflective space suggesting the presence of fluid was detected within the space of the cavitation in the OCT images (Figure 2 Second row, middle and right; and Third row, right). There was a direct communication between the vitreous cavity and the intrachoroidal cavitation in these 3 eyes (Figure 2 Third row, middle). In the area of macular in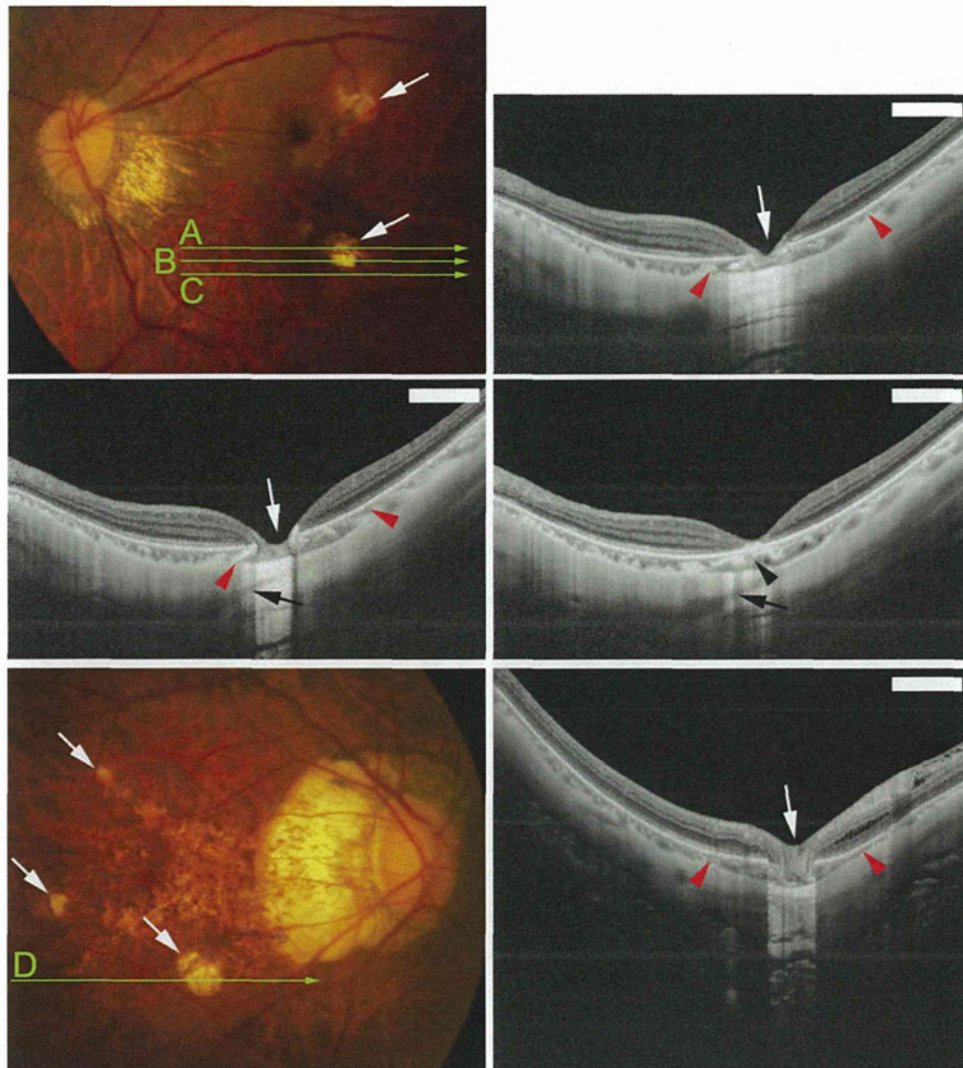trachoroidal cavitation, the choroid was thicker than that of the surrounding area; however, a close inspection of the OCT images showed a linear reflectivity near the inner surface of the intrachoroidal cavitation that may represent the original thickness of the choroid (Figure 3 Middle, right). This suggested that the cavitation, at least in some eyes, begins in the suprachoroidal space.

The average number of macular intrachoroidal cavitations/eye was $1.31 \pm 0.53$, with a range of 1 to 4. The total number of the different types of lesions in highly myopic eyes with patchy atrophy was 104, of which 41 (39.4%) were macular cavitations. In the 104 lesions, 1 of 4 lesions (25.0%) were located in the upper nasal quadrant, 4 of 17 lesions (23.5%) in the lower nasal quadrant, 7 of 27 lesions (25.9%) in the upper temporal quadrant, and 29 of 56 lesions (51.8%) in the lower temporal quadrant. Statistical analyses showed that the intrachoroidal cavitation developed significantly more frequently in the lower temporal quadrant than in the lower nasal or upper temporal quadrants ($P = .04$ and $P = .02$, respectively, by $\chi^2$ tests).

Statistical examinations showed that the patients with macular intrachoroidal cavitations were significantly older and the axial lengths of their eyes were significantly longer than those without these lesions (Table 2). The incidence of peripapillary intrachoroidal cavitations in eyes with macular intrachoroidal cavitations did not differ significantly from that of eyes without macular cavitations. The average size of patchy atrophy in eyes with macular intrachoroidal cavitations was $1.61 \pm 1.74$ mm$^2$, with a range of 0.195 to 8.50 mm$^2$, which was not significantly different from that of patchy atrophy without macular cavitation, at $1.53 \pm 2.05$ mm$^2$ with a range of 0.03 to 9.08 mm$^2$ ($P > .05$; Mann-Whitney $U$ tests). The width and depth of the macular intrachoroidal cavitation varied; however, the size of the intrachoroidal cavitation was larger than the RPE defects detected by OCT, and the intrachoroidal cavitations were larger than the area of patchy atrophy ophthalmoscopically (Figures 2 through 4). The average width of a macular intrachoroidal cavitation including the posterior displacement of the scleral curvature was $1568.0 \pm 776.3$ μm, with a range of 611 to 4411 μm. In 3 eyes, 2 separate intrachoroidal cavitations were fused at a deeper level and formed 1 large space (Figure 4). The intrachoroidal cavitation appeared very wide in these 3 eyes (widths of 2574, 3292, and 4411 μm). In 19 of 31 eyes (61.3%) with macular intrachoroidal cavitation, large

---

The indented appearance attributable to the caving-in of the retina into the intrachoroidal cavitation has a pseudo-fovea appearance (white arrow). (Third row, right) In the section shown by line E in top middle image, another intrachoroidal cavitation is observed (white arrow), and it is fused with the space of intrachoroidal cavitation. The sclera is bowed posteriorly (between arrowheads) and large intrascleral vessels (yellow arrow) are observed. The hyporeflectivity suggests the presence of fluid within the intrachoroidal cavitation. (Bottom) Three-dimensional (3D) rendered image of the retina. Perspective view was created by the 3D volumetric data set covering an area of 6 × 6 mm with 256 × 256 pixel density. Two caved-in pseudo-fovea-appearing structures are observed (arrows). Their locations are consistent with the patchy atrophy observed in the fundus images. (Bottom middle and Bottom right) Perspective cutaway view of the volumetric OCT data set at different transverse locations, showing 2 independent indentations (arrows) in the peripheral macula. The posterior sclera is bowed posteriorly and a part of the retina is caved into the intrachoroidal cavitation. Bar: 1 mm.

FIGURE 3. Small intrachoroidal cavitation with pseudo-fovea appearance. (Top left) Left fundus of a 55-year-old woman shows 2 areas of patchy chorioretinal atrophy (arrows). Her refractive error is −13.0 diopters and the axial length is 30.2 mm. (Top right) B-scan swept-source optical coherence tomographic (OCT) image of the scanned line A in top left image shows that the sclera is mildly bowed posteriorly (between arrowheads) beyond the area of retinal pigment epithelium (RPE) defects. The retina is caved into the space of intrachoroidal cavitation and has a pseudo-fovea appearance (arrow). A slight outer retinoschisis is observed around the patchy atrophy. (Middle left) In the section shown by line B in top left image, the posterior sclera is bowed posteriorly (between arrowheads) and the retina is caved into the intrachoroidal cavitation (white arrow). The linear hyporeflectivities suggestive of intrascleral vessels (black arrow) are observed in close proximity to the intrachoroidal cavitation. (Middle right) In the section shown by line C in top left image, a linear reflectivity (black arrowheads) is observed near the inner surface of intrachoroidal cavitation, which may represent the original thickness of the choroid. Large intrascleral vessels (black arrow) are observed in close proximity to the intrachoroidal cavitation. (Bottom left) Right fundus of a 65-year-old man showing 3 areas of patchy chorioretinal atrophy (arrows). His refractive error is −14.0 diopters and the axial length is 31.2 mm. (Bottom right) B-scan swept-source OCT image of the scanned line D in bottom left image shows that the sclera is bowed posteriorly (between arrowheads) beyond the areas of RPE defects. The retina is caved into the space of intrachoroidal cavitation and has a pseudo-fovea appearance (arrow). Outer and inner retinoschises are observed around the patchy atrophy. Bar: 1 mm.

intrascleral vessels were present very close to the area of the cavitation (Figures 2 and 4). An inner or outer retinoschisis was detected around the patchy atrophy in 22 of 33 eyes with a macular intrachoroidal cavitation (66.7%), which was significantly more frequent than in the 5 of 23 eyes without a cavitation (21.7%; $P = .0009$, $\chi^2$ test) or the 21 of 113 eyes without patchy atrophy (18.6%; $P < .0001$, $\chi^2$ test). An epiretinal membrane was found on and around the patchy atrophy in 11 of 22 eyes with retinoschisis and a macular intrachoroidal cavitation, and in 2 of 5 eyes with retinoschisis but without a cavitation. This difference was not significant.
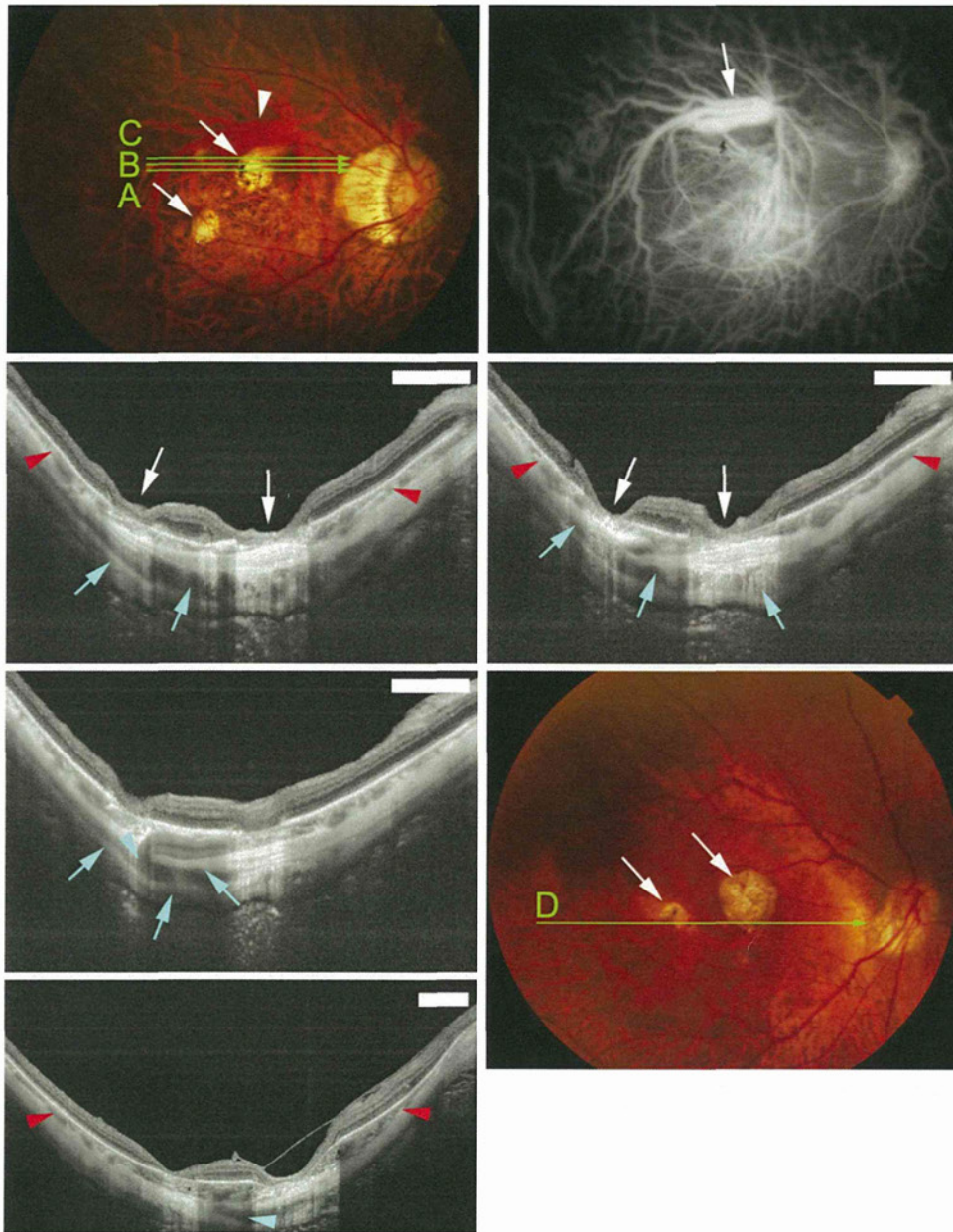
FIGURE 4. Presence of large posterior routes of choroidal blood outflow in close proximity to the space of intrachoroidal cavitation. (Top left) Photograph of the right fundus of a 74-year-old woman showing 2 areas of patchy chorioretinal atrophy (arrows). A large choroidal vein with ampulla (arrowhead) can be seen above the fovea. An intraocular lens was implanted in this eye, and the axial length is 29.6 mm. (Top right) Indocyanine green angiographic image at 7 minutes after dye injection shows a large choroidal vein with ampulla (arrow) above the fovea. (Second row left) B-scan swept-source optical coherence tomographic (OCT) image of the scanned line A in top left image shows the 2 areas of intrachoroidal cavitation (white arrows), and these 2 intrachoroidal cavitations fuse and form 1 large intrachoroidal cavitation. The scleral curvature is irregular (between arrowheads). A large intrascleral vessel can be seen (blue arrows). (Second row right) In the section shown by line B in top left image, large intrascleral vessels with branching can be seen (blue arrows). (Third row left) In the section shown by line C in top left image, large intrascleral vessels can be seen (blue arrows), with branching at the site shown by the arrowhead. (Third row right) Right fundus of a 70-year-old woman shows 2 areas of patchy chorioretinal atrophy above and temporal to the fovea (arrows). Her refractive error is −13.5 diopters and the axial length is 29.9 mm. (Bottom left) B-scan swept-source OCT image of the scanned line D in bottom right image shows the 2 areas of intrachoroidal cavitation (white arrows). The 2 areas are fused and form 1 large space. The sclera is bowed posteriorly between the arrowheads. The retina is caved into the space of intrachoroidal cavitation, and an epiretinal membrane and detachment of the inner limiting membrane is observed above the caved-in retina. Large intrascleral vessel (blue arrowhead) is observed in close proximity to the intrachoroidal cavitation. Bar: 1 mm.

**TABLE 2.** Comparison of Characteristics Between Highly Myopic Eyes With and Without Intrachoroidal Cavitation in the Macula

|  | Without Macular ICC | With Macular ICC | P Value |
|---|---|---|---|
| Number of eyes (persons) | 23 (14) | 31 (28) |  |
| Age (y), mean ± SD (range) | 57.3 ± 13.3 (30~79) | 64.3 ± 11.4 (36~79) | .026[a] |
| Axial length (mm), mean ± SD (range) | 29.6 ± 1.8 (29.0~35.3) | 30.8 ± 1.6 (27.1~32.7) | .046[a] |
| Peripapillary ICC | 2 eyes (8.7%) | 7 eyes (22.6%) | n.s. |

ICC = intrachoroidal cavitation; n.s. = not significant; SD = standard deviation; y = years.
[a]Mann-Whitney $U$ tests.

Among the 56 eyes, the morphologic features of the posterior pole in the swept-source OCT images in 2 eyes were very different from those of other patients. In these 2 eyes, the entire sclera was displaced posteriorly with an abrupt change in the scleral curvature in the area of the patchy atrophy (Figure 5). The color of the displaced area appeared orange to darkly pigmented and seemed to be excavated by stereoscopic fundus examinations. In 1 of these 2 eyes, the retina seemed to be torn away from the underlying sclera (Figure 5).

## DISCUSSION

OUR RESULTS SHOWED THAT INTRACHOROIDAL CAVITations were located in the macular area and on and around the patchy chorioretinal atrophy. Beneath the cavitation, the sclera was bowed posteriorly beyond the area of funduscopically observed patchy atrophy in 31 of 56 eyes (55.4%). The OCT features, the ophthalmoscopically observed orange color, and the fluorescein angiographic findings of the macular intrachoroidal cavitations were very similar to those of the peripapillary intrachoroidal cavitation.[13,15–17,22] However, the incidence of peripapillary intrachoroidal cavitation was not correlated with the presence of macular intrachoroidal cavitation.

In the area of a macular intrachoroidal cavitation, the choroid appeared to be thicker than that of the neighboring area. However, a close inspection of OCT images showed that a macular intrachoroidal cavitation, at least in some eyes, begins in the suprachoroidal space, as we reported for the peripapillary intrachoroidal cavitation.[13] Macular intrachoroidal cavitation can be differentiated from focal choroidal excavations[23–26] by the fact that focal choroidal excavations appeared to affect only the choroid and the sclera appears undisturbed in the enhanced-depth OCT images.[25]

Why does an intrachoroidal cavitation develop in the macular area away from the peripapillary region? The absence of macular intrachoroidal cavitation in any of the highly myopic eyes without patchy atrophy indicates that there is a close association of macular intrachoroidal cavitation to the areas of patchy atrophy. This relationship is similar to that between a peripapillary intrachoroidal cavitation and myopic conus. It is interesting that the histologic findings of myopic conus and patchy atrophy have many similarities: the RPE and choriocapillaris are absent in both lesions, and there is a destruction of the underlying Bruch membrane and photoreceptors in both types of lesions.[27,28] Even though the intraocular pressure is uniformly distributed on all walls of the eye, the expansion of the posterior wall should be more pronounced in the area of patchy atrophy or around a myopic conus because the absence of the retinal and choroidal layers makes this region thinner than the more normal regions away from the patchy atrophy. The thinner area should then be more susceptible to pressure.

Statistical analyses showed that highly myopic patients with macular intrachoroidal cavitation were significantly older and had significantly longer axial lengths than those without cavitation. These findings suggest that the patchy atrophy progresses to macular intrachoroidal cavitation with time and with further progression of myopia, although long-term longitudinal studies are necessary to confirm this hypothesis.

The OCT findings of macular intrachoroidal cavitation were also similar to those of small choroidal colobomas.[29] Gopal and associates[29] examined small choroidal colobomas with a Stratus OCT III and showed that the sclera appeared to be bowed posteriorly, as do macular intrachoroidal cavitations, although the image of the sclera was not clear with this type of OCT instrument (see their Figure 3). The swept-source OCT images of 1 of our patients with choroidal colobomas showed a posterior bowing of the sclera and the caving in of the retina into the space of the cavitation, as do macular intrachoroidal cavitations (Figure 6). Histologically, the normal choroid, RPE, and retina are absent in a colobomatous area, and these findings are also true in the areas of a myopic conus and patchy atrophy. Other than the difference in location, the major morphologic difference between a choroidal coloboma and myopic conus/patchy atrophy is whether the lesion is congenital or acquired. This would then suggest that highly myopic eyes can develop lesions that mimic a congenital anomaly because of the extensive elongation of the eye.
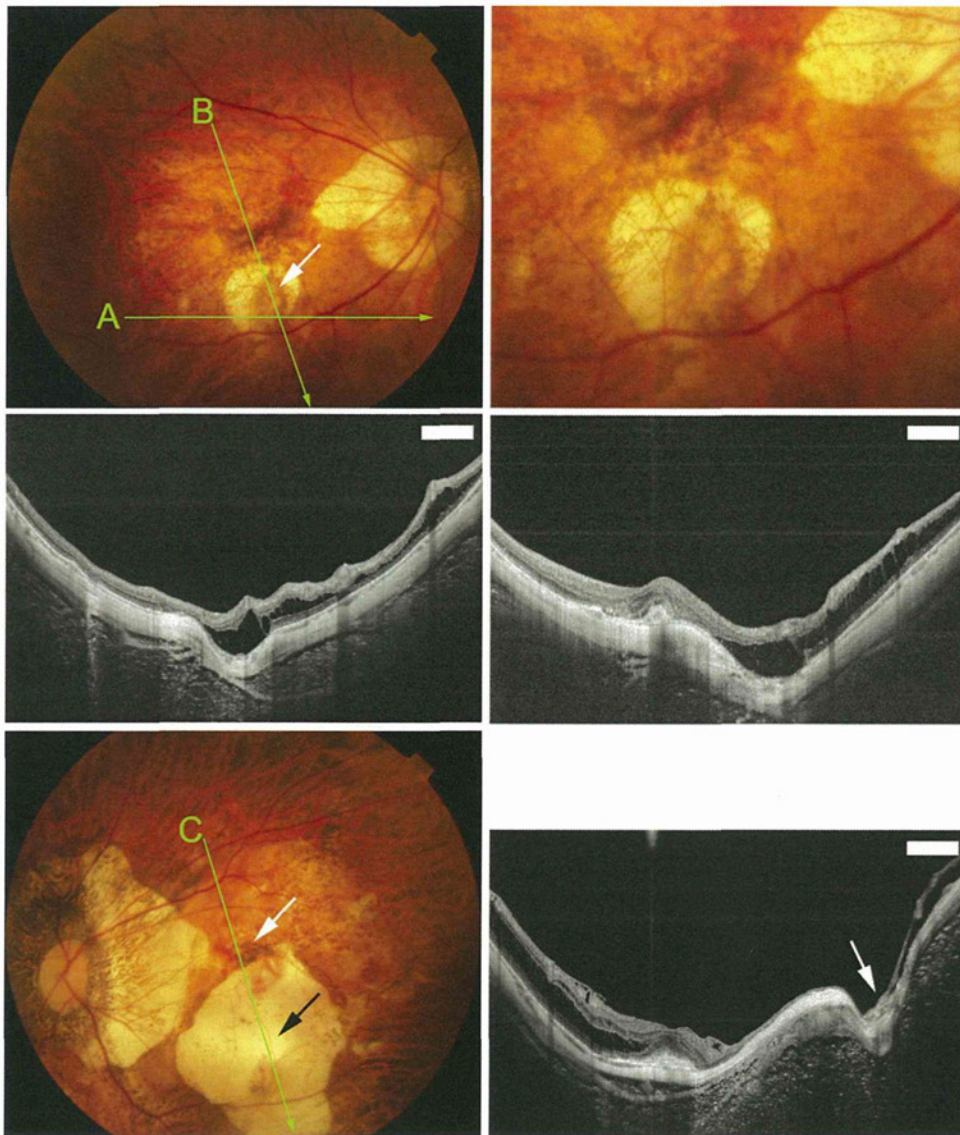
FIGURE 5. Posterior displacement of the entire scleral layer with an abrupt change in curvature of the neighboring sclera. (Top left) Right fundus of a 56-year-old woman with a large patchy chorioretinal atrophy inferior to the fovea. The central part of the patchy atrophy shows a grayish pigmentation (arrow). There is an intraocular lens implanted in this eye and the axial length is 30.2 mm. (Top right) Magnified view shows grayish pigmentation within the area of patchy atrophy. (Middle left) B-scan swept-source optical coherence tomographic (OCT) image of the scanned line A in top left image shows that the entire layer of sclera is displaced posteriorly, with an abrupt change in the curvature from the neighboring sclera. An outer retinoschisis is observed in and around the area of the patchy atrophy. The inner retina is torn away from the sclera with some tissue remnants in the subretinal space. (Middle right) B-scan OCT image of the scanned line B in top left image shows that the scleral curvature is irregular and distorted in the lower fundus. The entire layer of the sclera is displaced posteriorly, with an abrupt change in curvature from neighboring sclera. An outer retinoschisis is seen in the lower fundus, and the scar phase of a choroidal neovascular membrane is present in the fovea. (Bottom left) Photograph of the left fundus of a 72-year-old woman shows a large, patchy chorioretinal atrophy just inferior to the choroidal neovascular membrane (white arrow). The central area of patchy atrophy is pale (black arrow) compared to the other areas within the atrophy. (Bottom right) B-scan swept-source OCT image of the scanned line C in bottom left image shows that the entire layer of the sclera is displaced posteriorly, with an abrupt change in curvature from the neighboring sclera (arrow). The contour of the posterior sclera is irregular and severely distorted. The retina overlying the displaced sclera is extremely thin, and a retinoschisis is observed in the wide area of the fundus. Bar: 1 mm.

Large intrascleral vessels were found in close proximity to the area of macular intrachoroidal cavitation in 19 of 31 eyes (61.3%). Whether there is a causative relationship between the presence of such a large vessel within the sclera and the development of macular intrachoroidal cavitation is not clear. However, it might be possible that
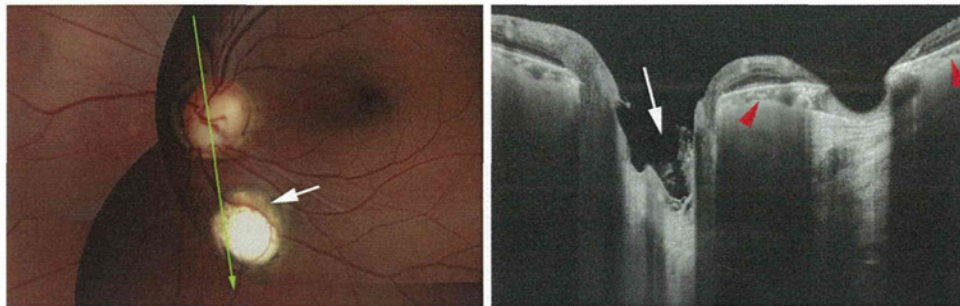
FIGURE 6. Swept-source optical coherence tomographic (OCT) images of choroidal coloboma. (Left) Photograph of left fundus of 53-year-old man shows choroidal coloboma inferior to the optic disc (arrow). (Right) B-scan swept-source OCT image of the scanned line in left image shows that the sclera is bowed posteriorly with a smooth change in curvature from the neighboring sclera (between arrowheads). The choroid appears to be thickened and the retina is caved into the space. The optic disc is excavated because of the accompanying disc coloboma (arrow).

the elasticity and rigidity of the sclera in the area adjacent to such large intrascleral vessels within thin sclera of highly myopic eyes might be reduced. When patchy atrophy develops in the area adjacent to large intrascleral vessels, the sclera in that area might be more susceptible to expansive forces.

We have reported that a macular retinoschisis was observed significantly more frequently in highly myopic eyes with advanced chorioretinal atrophy.[30] The present study using swept-source OCT showed that even among the highly myopic eyes with patchy atrophy, the eyes with macular intrachoroidal cavitation had retinoschisis around the patchy atrophy significantly more frequently than the eyes without cavitation. In the area of patchy atrophy, the inner retina appeared to be directly attached to the underlying sclera or remnants of the choroid subsequent to the development of intrachoroidal cavitation. The retina was then sunken into the space of cavitation. These observations suggest that the development of macular intrachoroidal cavitation might facilitate the dissociation of the retinal tissue in the area where the attachment between inner retina and sclera is considered to be weak. Thus, in addition to a weak adhesion between inner retina and underlying sclera, the mechanical dissociation attributable to the scleral bowing and the caving-in of the retina might facilitate the development of retinoschisis in and around the patchy atrophy.

Our data showed that macular intrachoroidal cavitation developed significantly more frequently in the patchy atrophic areas situated in the lower temporal quadrant than in the lower nasal or upper temporal quadrants. Actually, an intrachoroidal cavitation existed in 51.8% of the lesions with patchy atrophy located in the lower temporal quadrant. The reason for this preferential location is not fully known; however, one possibility is that this area might be the area most stretched by a staphyloma. This theory needs to be examined in the future. Chen and associates recently reported the presence of paravascular linear retinal breaks over the area of patchy chorioretinal

atrophy causing rhegmatogenous retinal detachments in 10 highly myopic eyes.[31] Unfortunately, the scleral curvature in these patients was not examined by swept-source OCT. They also found that the retinal breaks over the patchy atrophy were most frequently found along the inferotemporal vascular arcade.

In 2 of our patients, the sclera was not smoothly bowed out but only a part of the area with patchy atrophy was dislocated posteriorly, with an abrupt change of curvature (Figure 5). As a result, the scleral curvature in the posterior fundus in these 2 eyes was irregular and distorted (Figure 5). It is not known if the findings in these 2 eyes progressed from macular intrachoroidal cavitation or from patchy atrophy. In 1 of these 2 eyes, the retina appeared to be torn away from the underlying sclera.

Regardless of whether the scleral curvature changes smoothly or abruptly, our results showed that the scleral curvature was deformed in the area with patchy atrophy in a total of 33 of 56 (58.9%) of the eyes. This suggests that the patchy atrophy is clinically important not only as the cause of the absolute scotoma, but also as the cause of the deformation of the scleral curvature in a much wider extent beyond the area of patchy atrophy. As was recently shown in dome-shaped maculas,[32,33] the curvature of the sclera in the posterior fundus of highly myopic eyes appeared to be more complex than the 10 types of staphylomas reported by Curtin.[34]

There are several limitations to the present study. The number of highly myopic patients with patchy atrophy was not so high. Because the axial length in the highly myopic eyes without patchy atrophy was significantly shorter than in the eyes with patchy atrophy, the influence of axial length on the development of macular intrachoroidal cavitation cannot be completely excluded. Also, there were no follow-up data using swept-source OCT. Thus, it is not clear how macular intrachoroidal cavitations develop in the area of patchy atrophy and how they progress. Regardless of these limitations, the advancement of swept-source OCT,

which makes the observation of deeper tissue in vivo possible, has enabled us to discover a new pathology in eyes with pathologic myopia.

In conclusion, our results showed that a macular intrachoroidal cavitation was found in 55.4% of highly myopic eyes with patchy chorioretinal atrophy of the retina, and none was found in eyes without patchy chorioretinal atrophy. This suggests that patchy chorioretinal atrophy can affect the scleral contour in the area of a posterior staphyloma.

# REFERENCES

1. Krumpaszky HG, Ludtke R, Mickler A, Klauss V, Selbmann HK. Blindness incidence in Germany. A population-based study from Wurttemberg-Hohenzollern. Ophthalmologica 1999;213(3):176–182.

2. Munier A, Gunning T, Kenny D, O'Keefe M. Causes of blindness in the adult population of the Republic of Ireland. Br J Ophthalmol 1998;82(6):630–633.

3. Cotter SA, Varma R, Ying-Lai M, Azen SP, Klein R. Causes of low vision and blindness in adult Latinos: the Los Angeles Latino Eye Study. Ophthalmology 2006;113(9):1574–1582.

4. Buch H, Vinding T, La Cour M, Appleyard M, Jensen GB, Nielsen NV. Prevalence and causes of visual impairment and blindness among 9980 Scandinavian adults: the Copenhagen City Eye Study. Ophthalmology 2004;111(1):53–61.

5. Iwase A, Araie M, Tomidokoro A, Yamamoto T, Shimizu H, Kitazawa Y. Prevalence and causes of low vision and blindness in a Japanese adult population: the Tajimi Study. Ophthalmology 2006;113(8):1354–1362.

6. Xu L, Wang Y, Li Y, Cui T, Li J, Jonas JB. Causes of blindness and visual impairment in urban and rural areas in Beijing: the Beijing Eye Study. Ophthalmology 2006; 113(7):1134.e1–11.

7. Vongphanit J, Mitchell P, Wang JJ. Prevalence and progression of myopic retinopathy in an older population. Ophthalmology 2002;109(4):704–711.

8. Hayashi K, Ohno-Matsui K, Shimada N, et al. Long-term pattern of progression of myopic maculopathy: a natural history study. Ophthalmology 2010;117(8):1595–1611, 1611.e1591–1594.

9. Shih YF, Ho TC, Hsiao CK, Lin LL. Visual outcomes for high myopic patients with or without myopic maculopathy: a 10 year follow up study. Br J Ophthalmol 2006;90(5):546–550.

10. Ito-Ohara M, Seko Y, Morita H, Imagawa N, Tokoro T. Clinical course of newly developed or progressive patchy chorioretinal atrophy in pathological myopia. Ophthalmologica 1998;212(1):23–29.

11. Yun SH, Bouma BE. Wavelength swept lasers. In: Drexler W, Fujimoto JG, editors. Optical coherence tomography: technology and applications. New York: Springer, 2008: 359–377.

12. Hirata M, Tsujikawa A, Matsumoto A, et al. Macular choroidal thickness and volume in normal subjects measured by swept-source optical coherence tomography. Invest Ophthalmol Vis Sci 2011;52(8):4971–4978.

13. Spaide RF, Akiba M, Ohno-Matsui K. Evaluation of peripapillary intrachoroidal cavitation with swept source and enhanced depth imaging optical coherence tomography. Retina. Forthcoming.

14. Ohno-Matsui K, Akiba M, Moriyama M, Ishibashi T, Tokoro T, Spaide RF. Imaging the retrobulbar subarachnoid space around the optic nerve by swept source optical coherence tomography in eyes with pathologic myopia. Invest Ophthalmol Vis Sci 2011;52(13):9644–9650.

15. Shimada N, Ohno-Matsui K, Yoshida T, et al. Characteristics of peripapillary detachment in pathologic myopia. Arch Ophthalmol 2006;124(1):46–52.

16. Freund KB, Ciardella AP, Yannuzzi LA, et al. Peripapillary detachment in pathologic myopia. Arch Ophthalmol 2003; 121(2):197–204.

17. Toranzo J, Cohen SY, Erginay A, Gaudric A. Peripapillary intrachoroidal cavitation in myopia. Am J Ophthalmol 2005;140(4):731–732.

18. Yoshida T, Ohno-Matsui K, Yasuzumi K, et al. Myopic choroidal neovascularization: a 10-year follow-up. Ophthalmology 2003;110(7):1297–1305.

19. Yoshida T, Ohno-Matsui K, Ohtake Y, et al. Long-term visual prognosis of choroidal neovascularization in high myopia: a comparison between age groups. Ophthalmology 2002;109(4):712–719.

20. Williams TD. Determination of the true size of an object on the fundus of the living eye. Optom Vis Sci 1992;69(9):717–720.

21. Garway-Heath DF, Rudnicka AR, Lowe T, Foster PJ, Fitzke FW, Hitchings RA. Measurement of optic disc size: equivalence of methods to correct for ocular magnification. Br J Ophthalmol 1998;82(6):643–649.

22. Wei YH, Yang CM, Chen MS, Shih YF, Ho TC. Peripapillary intrachoroidal cavitation in high myopia: reappraisal. Eye 2009;23(1):141–144.

23. Abe S, Yamamoto T, Kirii E, Yamashita H. Cup-shaped choroidal excavation detected by optical coherence tomography: a case report. Retin Cases Brief Rep 2010;4:373–376.